

Low Voltage Controlled Fast Switchable Liquid Crystal-Based Reflectarray With Transverse Rubbing Layer

Hogyeom Kim, *Student Member, IEEE*, Jae-Won Lee, *Student Member, IEEE*, Seungwoo Bang, *Student Member, IEEE*, Junkai Wang, *Student Member, IEEE*, Min-Seok Kim, *Student Member, IEEE*, Hak-Rin Kim, *Member, IEEE*, and Jungsuek Oh, *Senior Member, IEEE*

Abstract— This paper proposes a low voltage controlled fast beam switchable liquid-crystal-based reflectarray (LC-RA). By introducing a strip array of ground patterns and a transverse rubbing layer, a 1.5 V-powered falling response can be achieved for fast beam switching. Typically, the falling response of the LC cannot be controlled by the bias voltage, leading to slow beam switching. The strip array, in conjunction with the top electrodes, generates lateral fields for arranging the molecules of the LC, enabling the falling nature to be controlled by the bias voltage. In addition, the transverse rubbing layer achieves a low voltage-based fast-falling response without degradation of antenna performance. This study demonstrates the antenna performance and switching speed of the proposed LC-RA and compares it with other LC-based antennas. Finally, the proposed antenna achieves 1.6 sec of switching speed with under bias voltage of 5 V for the beamforming. Moreover, the proposed design shows high antenna performance, such as aperture efficiency, SLL, and scanning range, compared to the LC-based antennas at the mmWave band.

Index Terms— Fast beam switching, liquid crystals, reconfigurable reflectarray antenna.

I. INTRODUCTION

Liquid crystal (LC) based-antenna has been actively studied and utilized owing to its versatile applications, such as polarization converter, polarizer, and phase modulator [1-4]. There are main advantages of the LC, including phase continuity, low power consumption, and operating spectrum. However, the LC-based antennas suffer from low response speed due to their viscosity nature. To solve this problem, many kinds of research have employed thin LC layers or the establishment of polymer network LC (PNLC) or dual-frequency LC to enhance response speed [5-8].

This research was supported by the Challengeable Future Defense Technology Research and Development Program through the Agency for Defense Development (ADD) funded by the Defense Acquisition Program Administration in 2023 (No.915021201). (Hogyeom Kim and Jae-Won Lee contributed equally to this work. Hak-Rin Kim and Jungsuek Oh contributed equally to this work.) (Corresponding author: Jungsuek Oh.)

Hogyeom Kim, Seungwoo Bang, and Jungsuek Oh are with the Institute of New Media and Communication (INMC) and the Department of Electrical and Computer Engineering, Seoul National University, Seoul 08826, South Korea (e-mail: jungsuek@snu.ac.kr).

Hak-Rin Kim is with the School of Electronics Engineering and the School of Electronic and Electrical Engineering, Kyungpook National University, Daegu 41566, South Korea (Co-corresponding author's e-mail: rineey@knu.ac.kr).

Jae-Won Lee, Junkai Wang, and Min-Seok Kim are with the School of Electronic and Electrical Engineering, Kyungpook National University, Daegu 41566, South Korea.

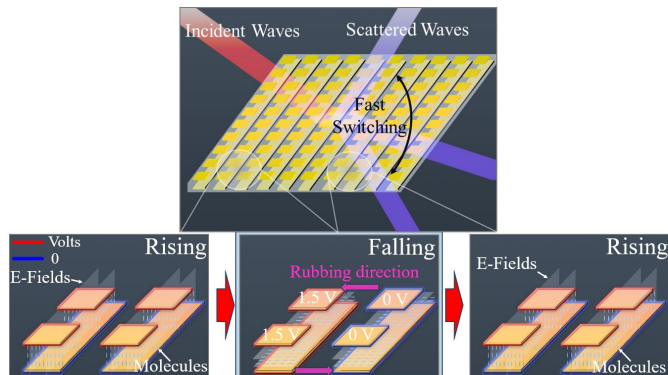


Fig. 1. The concept of the proposed design and beamforming process.

However, these solutions deteriorate the performance of LC-based antenna, including phase shift range and increase RF loss.

This paper proposes fast switchable LC-based reflectarray (LC-RA) by introducing a low-voltage based bias scheme. Two design methodologies achieve fast beamforming. Firstly, the ground pattern of the LC-RA is established using a strip array configuration. Secondly polyimide should be rubbed along the transverse direction of the ground pattern. Conventional LC-based antennas typically apply the polyimide along the intended polarization vector, but not this study [9]. The fact that the polyimide layer does not affect the antenna performance is demonstrated by this study.

Fig.1 depicts the concept of the proposed design and continuous beamforming process. The beamforming is accomplished by the conventional method, denoted as rising. Subsequently, the beam switching is accelerated by applying low voltage of 1.5 V to each top patch and ground electrode and zero voltage to adjacent top and bottom electrodes, denoted as falling, thereby enabling fast beam switching. Low-voltage systems relieve the burden associated with establishing a high-voltage control circuit system. The enhancement of the proposed method will be compared to the conventional beam switching in this study. Finally, the switching time is improved by 2.02 times faster than the conventional field-cut-off method without degradation of antenna performance. The proposed antenna achieves 38.9 % of aperture efficiency, -15.3 dB of SLL, and 100° of beam coverage.

The remainder of this paper is organized as follows. In Section II, design and simulation results versus anisotropic permittivity are presented.

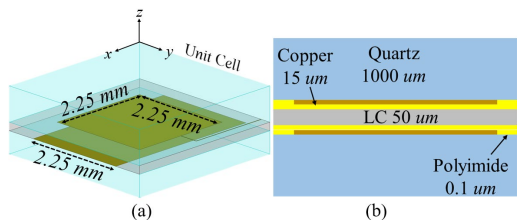


Fig. 2. (a) the proposed unit cell and (b) a side view of the unit cell.

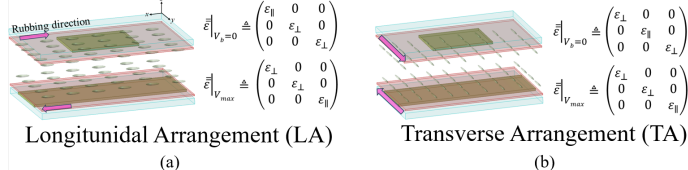


Fig. 3. (a) Conventional longitudinal arrangement and (b) transverse arrangement and corresponding permittivity tensors.

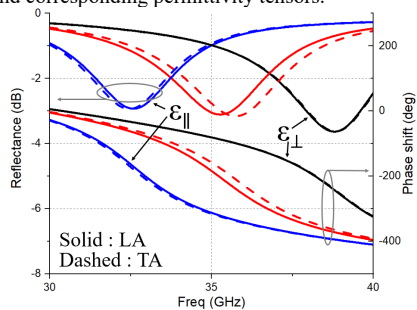


Fig. 4. Frequency responses versus anisotropic permittivity of two arrangement cases.

In Section III the measured results and beam switching characteristics of the proposed LC-RA are discussed.

II. THE PROPOSED LC-RA DESIGN

A. Operation Principle of the Proposed LC-RA

This section introduces the proposed LC-RA design from unit cell to full array design. Frequency simulation is conducted from the full-wave simulator, HFSS to confirm unit cell performance versus anisotropic LC.

Fig. 2(a) and (b) illustrate the proposed unit cell of this study. A 1000 um thickness of quartz glass is employed for the substrate. Copper deposition was processed on both sides of the LC to resonate the RF waves and excite the LC. The ground pattern of the proposed unit cell has the same width as the patch electrode. The periodicity of the unit cell is 3 mm. The square patch dimensions and the width of the ground pattern are 2.25 mm. In this study, the polyimide layer is rubbed along the x - or y -axis to achieve the desired rubbing effect on the dynamic nature. The GT7 LC (Merck KGaA, Darmstadt, Germany) was used in this study. The relative permittivity of the LC has a complex value ($\epsilon'_{LC} - j\epsilon''_{LC}$) owing to its loss feature. Based on the datasheet, the tunable range of the dielectric constant of the LC used in this study is expected to be 2.46–3.56 (from ϵ_{\perp} to ϵ_{\parallel} at 19 GHz) and the corresponding loss tangent decreases from 0.012 to 0.0064. The cell gap of the LC was chosen to be 50 um. The dielectric constant and loss tangent of quartz glass are 3.9 and 0.0004, respectively.

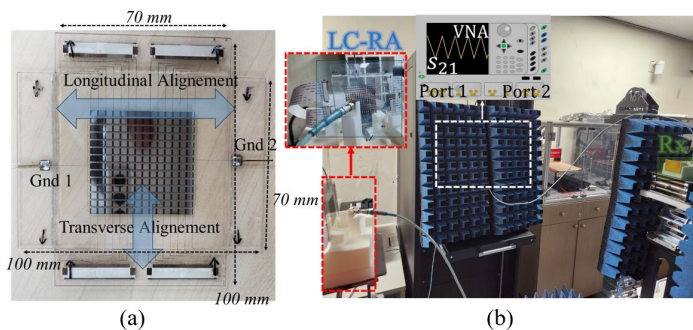


Fig. 5. (a) Fabricated sample and (b) the measurement setup.

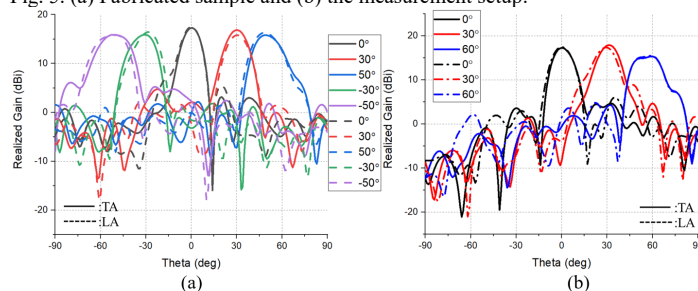


Fig. 6. Measured results of the (a) H-plane and (b) E-plane beam patterns for TA and LA cases.

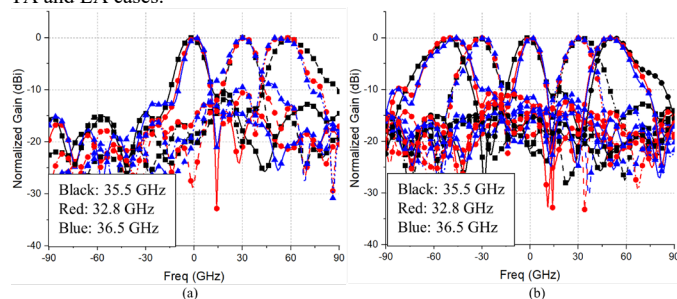


Fig. 7. Pattern bandwidth. ((a) H-plane and (b) E-plane)

Fig. 3 shows two arrangement cases used in the LC-RA. The conventional LA case is intended to align with the desired wave polarization. However, this study employs the TA case for the fast beam switching with low voltage. According to the two extreme bias states, the permittivity tensor of two cases is shown in Fig. 3.

Fig. 4 shows frequency responses according to the effective permittivity of two anisotropic LCs. Solid and dashed lines present LA and TA cases, respectively. The results confirm that the performance of the unit cell is primarily influenced by the z -components of the tensor [10]. The maximum reflection loss and phase shift range at 35.5 GHz are 3.3 dB and -260° , respectively.

B. Discuss on the Measured Results

This section discusses the measured results of beam patterns and switching characteristics. Fig. 5(a) depicts a fabricated sample of the proposed LC-RA which consists of 196 pins for exciting unit cells and two ground pins. In this study, measurement results, such as beam patterns and switching speed, of two alignment cases are discussed. Fig. 5(b) shows the measurement environment and beam switching process. The 2×2 patch array antenna is employed as a feed antenna to reduce the blockage loss [11]. Focal length and feeding offset angle are 30 mm and 30° , respectively.

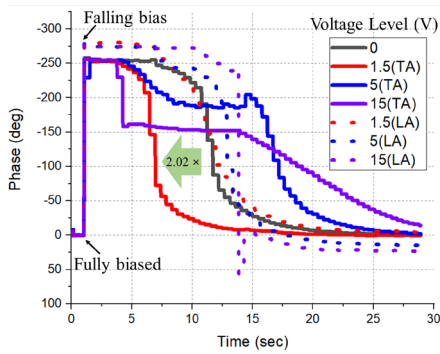


Fig. 8. Measured falling time of two alignment cases versus bias voltage.

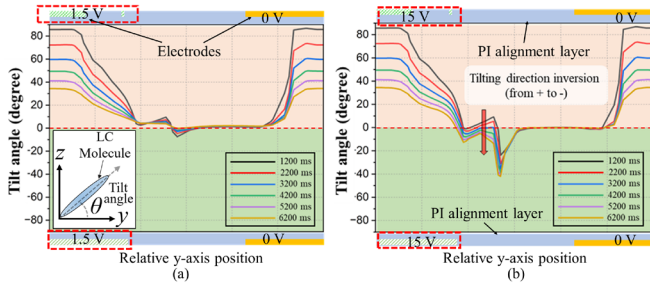


Fig. 9. Dynamic characteristics of lateral LC director profiles of the cell with the TA during the falling response by (a) 1.5 V and (b) 15 V, where the time-dependent lateral distributions of the LC tilting angles are co-plotted after sampling at the depth position of $z = 30 \mu\text{m}$ within the LC cell.

In the measurement system, the multi-channel control circuit board is employed to provide voltages ranging from 0 V to 5 V.

Fig. 6 shows the measured results of the beam pattern for two alignment cases. In the H-plane, the measured gain ranged from 15.7 to 17.3 dBi, with a beam coverage range of -50° to 50° . In the E-plane, the measured beam patterns ranged from 15.4 to 17.9 dBi, with a beam coverage range of 0° to 59° . The maximum sidelobe level was confirmed as -15.3 dB.

Fig. 7 shows the pattern bandwidth (BW) of the proposed LC-RA. The BW was evaluated by considering radiation patterns, acceptable SLL, and steering angle. The pattern BW of the proposed structure has been confirmed to be 3.7 GHz.

Fig. 8 shows the measured falling time of two alignment cases versus bias voltage. It should be noted that in the fully biased case, the resolution of the VNA employed in the experiment does not guarantee precise fully biased time. Therefore, the fully biased time of the proposed LC-RA is expected to be under 30 msec considering the measurement limitation. The falling time was evaluated from the moment when the falling bias was applied to the time when the phase reached 90 % of the saturated phase. The conventional falling time, when all bias voltage is cut off, is 11.9 sec, and it is maximally enhanced to be 2.02 times faster through the proposed bias configuration with transverse rubbing. As shown in Fig. 9, the falling response of the LC can be controlled by bias voltage. The falling time of the TA dramatically varies with changes in bias voltage, unlike in LA cases. There is an abrupt phase change 2.72 sec after the falling bias is applied.

In TA cases, the falling time increases as the bias level rises, as illustrated in Fig. 8. The LC dynamics were analyzed in detail using the TechWiz LCD 3D simulator. Fig. 9 depicts the dynamic characteristics of the LC director profiles during falling bias with varying bias voltage levels.

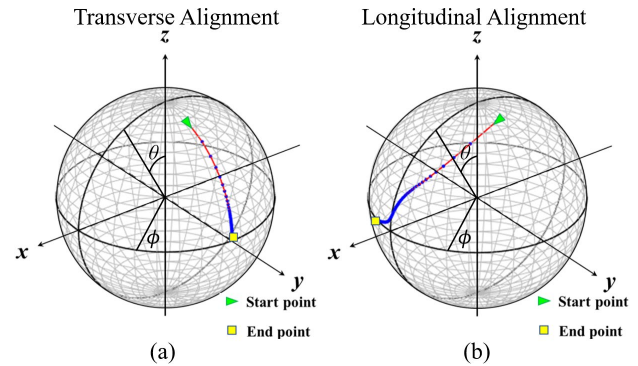


Fig. 10. Dynamic trajectories of LC director where the azimuth (ϕ) and polar (θ) angles of time-evolving LC director, $n(\phi, \theta)$ are plotted on the unit spherical surface. For (a) the TA and (b) the LA cases are operated by the falling bias with 1.5 V. The analyzed LC director sampling position is at the depth position of $z = 40 \mu\text{m}$ below top electrode. The blue circles are plotted with the same time interval of 200 msec.

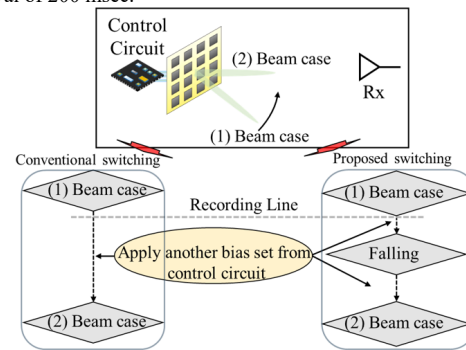


Fig. 11. Beam switching test processes with and without the proposed bias configuration.

When operated with a 15 V bias, the dynamics of the LC exhibit changes in tilting, including an inversion in the tilting direction. This inversion also occurs in the lateral direction, resulting in an abrupt phase change, as illustrated in Fig. 9(b).

$$\varepsilon_{eff}(V) = \frac{\varepsilon_{\perp} \varepsilon_{\parallel}}{\sqrt{\varepsilon_{\perp}^2 \sin^2(\theta_{LC}) + \varepsilon_{\parallel}^2 \cos^2(\theta_{LC})}} \quad (1)$$

where the θ_{LC} represents the tilt angle. The effective permittivity ε_{eff} can be defined as (1), and the overshoot, such as tilting angle inversion for the 15 V bias case, affects abrupt phase change.

The LC-RA cell with the TA case can be stabilized with changes in the polar angle of the LC director under optimal bias conditions, while the LC director trajectory of the LC-RA cell with the LA case accompanies variations in both ϕ and θ , as shown in Fig. 10.

In Fig. 11, the beam switching test setup is shown. LC-based antennas suffer from slow beam switching due to the inherent field-off nature of the LCs. To enhance beam switching speed, the proposed bias configuration is introduced during beam switching. The TA-based LC-RA was chosen as the test sample. The switching evaluation is processed as follows:

1. Set the Rx antenna toward the direction where the beam points for the 2) case.
2. Apply bias set for the 1) beam case.
3. Record the S_{21} parameters using the VNA, then apply the bias set for the 2) beam case.

Table I

Comparison of the beam-switching time w/o and w/ the falling bias.

		1) Beam case (sec)		
		0	30	50
w/o	0	-	8.4	7.4
	30	8.5	-	8.2
	50	7.9	7.8	-
w/	0	-	1.7	2.2
	30	2.3	-	1.6
	50	2.1	2.2	-

TABLE II

Performance comparison of LC-based antennas

Feature	Ref. [9]	Ref. [12]	Ref. [13]	Ref. [15]	Ref. [16]	This work
Frequency [GHz]	17.5	37.5	20	104	110	35.5
Aperture Efficiency [%]	13.8	22.9	N.A.	N.A.	N.A.	38.9
SLL [dB]	-4	-14	N.A.	N.A.	N.A.	-15.3
Scanning Capability	2D	2D	N.A.	N.A.-	N.A.	2D
Scanning Range [°]	50	35	N.A.	N.A.	N.A.	100
Max. Bias Level (V)	15	36	40	24	20	5
Switching Speed (sec)	150	6.05	3	*0.13	*0.19	1.6
LC thickness (um)	100	200	10	30	65	50
Frequency Tunability (%)	N.A.	5.9	N.A.	3.6	4.4	15
Radiation BW (GHz)	N.A.	N.A.	N.A.	N.A.	N.A.	3.7

*The results were measured in the field of optics, which may not fully represent RF switching time.

4. Evaluate the switching time when the S_{21} parameter reaches the gain of the corresponding beam.

5. Compare the switching time with and without the proposed bias configuration.

Table I shows the measured beam-switching time with and without the falling bias configuration. Without falling bias, the fastest beam-switching time is 7.4 sec. In the case with falling bias, a 1.5 V in-plane bias set is employed, resulting in a maximally fast beam-switching time of 1.6 sec, which is more than 4.6 times faster than the field-off time without falling bias. In these results, the beam-switching speed is faster than the falling bias because some of the bias sets for beamforming include rising bias.

Table II shows the performance comparison of LC-based antennas investigated in the mmWave band. This study achieves low voltage-based fast-beam switchable characteristics with reliable antenna performance, such as high aperture efficiency, SLL, and scanning range. Although [15] and [16] report switching speed of 0.13 and 0.19, respectively, their results were measured in the field of optics. These measurements may not fully represent the RF domain because the polarizer in the test setup allows only single-polarized waves, whereas complex local fields exist in the RF domain.

III. CONCLUSION

This study proposed an LC-RA with a low voltage controlled fast beam switchable characteristic. By introducing a strip array of ground patterns and utilizing transverse rubbing direction, the falling response was enhanced by 2.02 times compared to

the conventional method with 1.5 V of voltage. The mechanism of the LC molecules was analyzed in detail using an LC simulator. Finally, this study achieved a maximum beam switching speed of 1.6 sec, the fastest speed compared to the other LC-based antennas. Moreover, the proposed design shows high antenna performance.

ACKNOWLEDGMENT

The authors would like to thank Prof. Seongwoog Oh for helping with the measurement of the beam switching time.

REFERENCES

- [1] L. Wei, T. T. Alkeskjold and A. Bjarklev, "Compact Design of an Electrically Tunable and Rotatable Polarizer based on a Liquid Crystal Photonic Bandgap Fiber," *IEEE Photon. Techn. Lett.*, vol. 21, no. 21, pp. 1633-1635, Nov.1, 2009.
- [2] T. Sasak, Y. Nishie, M. Kambayashi, M. Sakamoto, K. Noda, H. Okamoto, N. Kawatsuki and H. Ono, "Active Terahertz Polarizer Converter Using a Liquid Crystal-Embedded Metal Mesh," *IEEE Photon. J.*, vol. 11, no. 6, pp. 1-7, Dec. 2019.
- [3] J. Kim, W. Lee and J. Oh, "Liquid-Crystal-Tuned Resonant Series Patch Array with Unique Element Spacing Emulating Simplified Operating Construe of Traveling-wave Antenna," *IEEE Antennas Wireless Propag. Lett.*, early access.
- [4] W. Zhang, Y. Li, and Z. Zhang, "A reconfigurable reflectarray antenna with an 8- μ m-thick layer of liquid crystal," *IEEE Trans. Antennas Propag.*, vol.70, no. 4, pp. 2770-2778, April 2021.
- [5] D. C Zografopoulos and R. Beccherelli, "Tunable terahertz fishnet meta materials based on thin nematic liquid crystal layers for fast switching," *Sci. Rep.*, vol. 5, p.13137, Aug. 2015.
- [6] R. Guirado, G. Perez-Palomino, M. Caño-García, M. A. Geday and E. Carrasco, "mm-Wave metasurface unit cells achieving millisecond response through polymer network liquid crystals," *IEEE Access*, vol. 10, pp. 127928-127938, 2022.
- [7] Y.-C. Shin, J.-S. Park, K.-I. Joo, R. Manda, J.-C. Choi and H.-R. Kim, "Optically isotropic liquid crystal mode templated by nanoporous breath figure membrane," *Adv. Mater. Interfaces* vol. 9, no. 7, Jan. 2022.
- [8] K.-I. Joo, M.-K. Park, H. Park, T.-H. Lee, K.-C. Kwon, Y.-T. Lim, M.-U. Erdenebat, H. Lee, G. Lee, N. Kim and H.-R. Kim, "Light-field camera for fast switching of time-sequential two-dimensional and three-dimensional image capturing at video rate," *IEEE Trans. Ind. Electron.*, vol. 67, no. 8, pp. 6975-6985, Aug. 2020.
- [9] H. Karabey, A. Gaebler, S. Strunck and R. Jakoby, "A 2-D electronically steered phased-array antenna with 2×2 elements in LC display technology," *IEEE Trans. Microw. Theory Techn.*, vol. 60, no. 5, pp. 1297-1306, May 2012.
- [10] T. -W. Kim, J. -S. Park and S. -O. Park, "A theoretical model for resonant frequency and radiation pattern on rectangular microstrip patch antenna on liquid crystal substrate," *IEEE Trans. Antennas Propag.*, vol. 66, no. 9, pp. 4533-4540, Sept. 2018.
- [11] H. Kim, J. Kim and J. Oh, "A novel systematic design of high-aperture-efficiency 2D beam-scanning liquid-crystal embedded reflectarray antenna for 6G FR3 and radar applications," *IEEE Trans. Antennas Propag.*, vol. 20, no. 10, pp. 1898-1902, Oct. 2021.
- [12] X. Li, H. Sato, H. Fujikake and Q. Chen, "Development of Two-dimensional steerable reflectarray with liquid crystal for reconfigurable intelligent surface application," *IEEE Trans. Antennas Propag.*, early access.
- [13] W. Hu, O. H. Karabey, A. Gäbler, A. E. Prasetiadi, M. Jost and R. Jakoby, "Liquid crystal varactor loaded variable phase shifter for integrated, compact, and fast beamsteering antenna systems," *2014 44th EUCAP*, Italy, 2014, pp. 1604-1607.
- [14] G. Deng, H. Mo, Z. Kou, J. Yang, Z. Yin, Y. Li, and H. Lu, "A polyimide-free configuration for tunable terahertz liquid-crystal-based metasurface with fast response time," *Optics & Laser Technology*, vol. 161, pp. 109127, 2023.
- [15] G. Deng, H. Mo, Z. Kou, J. Yang, Y. Li, Z. Yin, and H. Lu, "Design and experimental investigation of interdigitated electrode architecture for tunable liquid crystal-based metasurfaces with rapid responses," *Infrared Physics & Technology*, vol. 133, pp. 104768, 2023.